Effect of Toluene Diisocyanate Index on Morphology and Physical Properties of Flexible Slabstock Polyurethane Foams

DIMITRIOS V. DOUNIS, GARTH L. WILKES

Department of Chemical Engineering, Polymer Materials and Interfaces Laboratory, Virginia Polytechnic Institute and State University, Blacksburg, Virginia 24061-0211

Received 31 August 1996; accepted 8 April 1997

ABSTRACT: The effect of toluene diisocyanate (TDI) index on the physical properties, structure, and morphology of flexible slabstock polyurethane foams was investigated. Foams based on a 2700 molecular weight triol, 6 pph water, and varying amounts of an 80/20 mixture of 2,4- and 2,6-TDIs were characterized using a number of physical property and morphological measurements. Extraction experiments using dimethyl formamide (DMF) showed that increasing the index increased the level of covalent crosslinking with perhaps a maximum being reached at an index ca. 100. Viscoelastic measurements also supported the claim of increased crosslinking with TDI index. The initial load in load relaxation experiments at 65% strain systematically increased with increasing TDI while the percent decay in a 3-h period decreased. Temperature and/or humidity "plasticized" the load relaxation behavior in all the foams studied, indicating that the hard segment domain physical "crosslinks" play a significant role in the properties of these materials. Interestingly, compression set measurements appeared to be independent of the index, likely due to some level of hard segment continuity, but the induced recovery of the compression set at elevated temperatures was indeed sensitive to the index. The amount of recovery systematically increased with increasing TDI index due to the more enhanced "recoverable" covalent network. Scanning electron microscopy (SEM) studies of the foams showed that the cellular structure was not significantly affected by the index. However, SEM also showed that the structure of the high index foam was not greatly altered by the extraction process while the lowest index foam's cellular structure was severely disfigured. The fine structure of the foams was found to be influenced by the TDI index. Small angle X-ray scattering, differential scanning calorimetry, and dynamic mechanical analysis all provided evidence that an increase in the TDI index promoted some phase mixing of the soft and hard segments. FTIR showed that the short-range ordering within the hard segment domains displayed a maximum at an index of 100. This was attributed to the concentration of hard segment domains being lower at a lower index and their ordering being disrupted at higher indexes due to more extensive covalent crosslinking prior to completion of phase separation. Wide angle X-ray scattering results also confirmed that for the highest index level, the short-range ordering of the TDI moieties was decreased.
 J Appl Polym Sci **66:** 2395–2408, 1997

Key words: toluene diisocyanate index; flexible slabstock polyurethane foams; morphology; physical properties

Correspondence to: Prof. G. L. Wilkes (gwilkes@vtvmL.cc.vt.edu).

Journal of Applied Polymer Science, Vol. 66, 2395–2408 (1997)
 CCC 0021-8995/97/132395-14

INTRODUCTION

Polyurethane foams are used in a very wide range of applications that are primarily in the areas of

insulation, packaging, and load bearing such as cushioning. This broad application base inherently requires that foams be made with varying levels of "stiffness." Traditionally this was accomplished by the use of low boiling liquids or auxiliary blowing agents that influenced the density and softness of the foam. Chlorofluorocarbons (CFCs) were the most widely used auxiliary blowing agents. However, due to the concerns about the effects of CFCs on the ozone layer of the earth's atmosphere, these materials have been nearly phased out from the formulation of polyurethane foams. This has therefore led urethane foam manufacturers to alter foam formulations and derive novel components to meet the changing and evolving application base.

Many alterations in the formulation components are currently being investigated such as novel polyols, softening additives, crosslinking additives, hardening additives, and cell-opening additives. Modifications to the existing formulation components include altering polyol molecular weight, polyol functionality, isocyanate functionality, isocyanate molecular weight, isocyanate amount (isocyanate index), and the amounts of water, catalysts, surfactants, etc. In this study a new proprietary polyol (nominal functionality 3.15) was used in conjunction with a constant 6-pph water content. The isocyanate index was varied from 85 to 110.

In view of the trend to alter the chemical formulation of slabstock foams to meet the needed performance, there is also a need for obtaining a greater *fundamental* understanding of the relationships between the foam's structure–morphology and physical properties. For example, the network structure of a typical polyurethane foam is comprised of both chemical and physical "crosslinks." The chemical or covalent crosslinks arise from the use of a hydroxyl polyol of functionality greater than 2 while the physical crosslinks arise from the phase separated hard domains (urea segments). Although both types of crosslinks enhance the foam's physical properties, physical crosslinks are labile at high temperatures and high humidity, thus dramatically altering the foam's properties. The formulation used in this study includes a high water level (6 pph) and a varying isocyanate index. This is expected to bring about changes in the physical properties, morphology, and network structure, with the general trend being that as the isocyanate index is increased, the level of covalent crosslinking is also increased. It is also believed that as the level of covalent crosslinking is increased, the morphology (noncellular) is also influenced, decreasing the level of phase separation between the rigid high glass transition temperature (T_g) urea hard segment and the ether soft segment.

Although limited, some work does exist in the literature regarding the effect of crosslinking on the properties of segmented polyurethane materials. For example, Petrovic et al. introduced crosslinks into a segmented polyurethane elastomer based on 4,4′-diphenylmethane diisocyanate (MDI), by varying the ratio of poly(oxypropylene) diol to poly(oxypropylene/oxyethylene) triol.[1] They found that the tensile strength and tear strength was enhanced with an increasing level of crosslinking while the modulus was raised only at very high triol ratios. The stress relaxation rate initially decreased except at very high triol ratios where no change was observed in the relaxation rate. Based on these results and the insensitivity of the shear modulus in dynamic mechanical measurements to crosslinking, they concluded that the hard segment domains significantly contribute to (and may dominate) this particular mechanical property of these elastomers.

Ophir and Wilkes investigated the mechanical and phase separated structure on a series of segmented polyester–MDI polyurethane elastomers that were peroxide cured to introduce covalent crosslinking at a temperature sufficiently high where mixing occurred of the hard and soft segments.[2] They showed that as the level of crosslinking increased, the amount of phase separation decreased when the material was cooled to ambient. This was demonstrated using small angle X-ray scattering (SAXS) where the calculated invariant decreased and with differential scanning calorimetry (DSC) where the final soft segment glass transition temperature increased with increasing crosslinking due to phase mixing. Furthermore, they found that the Young's modulus also systematically decreased with increasing crosslinking. Because the increased covalent crosslinking provides a more phase mixed system, it prevents the complete cohesive packing of the hard segments into well ordered domains, thereby reducing their strengthening effect. In addition, the thermal stability was decreased with increasing crosslinking where the domain structure was more easily disrupted at a given temperature as the level of crosslinking increased.

Spathis et al. also studied morphological changes induced by crosslinking in segmented elastomeric polyurethanes based on MDI and poly(ethylene adipate) with butane diol as the chain extender.[3] In this case the level of crosslink-

ing was altered by varying the NCO/OH ratio in the second step of polymerization, which resulted in the formation of allophanate groups. FTIR studies showed that as they increased the NCO/OH ratio, they also increased the level of phase mixing and that the hydrogen bonded N—H and carbonyl absorbance decreased while the free absorbance increased in both cases. DSC results confirmed this with an increasing T_g with increasing NCO/OH ratio. Along with following the changes in the T_g, the authors noted a systematic decrease in the soft segment melting endotherm (ca. 50°C) with increasing NCO/OH ratio, again indicative of phase mixing.

Recently Thomas et al. investigated the effect of crosslinking on the morphology and thermal and mechanical properties of flexible molded polyurethane foams and films, based on a 4800 molecular weight propylene oxide–ethylene oxide blend, 4 pph water, and toluene diisocyanate (TDI).[4] They altered the level of covalent crosslinking by changing the functionality of the polyol that was accomplished by the addition of monofunctional polyether molecules. This decreased the functionality from 2.79 to 2.56. Although their FTIR results were insensitive to crosslinking at the levels studied, both SAXS and thermal analysis suggested that increasing the polyol functionality increased the phase mixing. The calculated values of the scattering invariant decreased as they increased the functionality in the analysis of the SAXS data and the specific heat change at the glass transition also decreased in the analysis of the DSC thermograms. In terms of mechanical properties, the elongation at break (in stress–strain experiments) decreased with increasing polyol functionality while the stress at break and Young's modulus was independent of functionality. The viscoelastic nature of these materials was also investigated with stress relaxation measurements from which the authors observed that increasing the polyol functionality decreased the relaxation rate.

Cavender and Hawker studied the effect of varying the isocyanate index on certain physical properties of TDI and MDI based automotive seating foam.[5] In general, they found that the tensile strength, 50% initial force deflection (IFD), tear strength, and compression set increased with an increasing index. The percent elongation, however, decreased with an increasing index.

In a recent study by Skorpenske et al.[6] the influence of TDI index on the physical properties of flexible slabstock polyurethane foams based on a 3000 molecular weight triol and 5-pph water content was investigated. The TDI index was varied from 85 to 105, which increased the level of crosslinking. Hard segment organization was determined through FTIR analysis of the amide I region (1800–1620 cm^{-1}). They found that the percent hydrogen bonding increased slightly but the hydrogen bonding index (degree of hard segment organization) increased systematically up to an index of 95, beyond which it systematically decreased. In terms of physical properties, the tensile, tear, resiliency, and elongation properties all displayed a maximum at an index of 100. The indentation load deflection results, however, continually increased with increasing index throughout the entire range. The authors also found that the compression set decreased with increasing index with the exception being at compression set temperatures above 105°C where the compression set results were independent of the index.

This article investigates the mechanical and viscoelastic behavior of flexible slabstock polyurethane foams as well as the structure and the morphology, all as a function of TDI index. The goal is to obtain a more fundamental understanding of the role TDI index plays in the morphology and physical properties.

EXPERIMENTAL

Materials

The formulation components used in this study are given in Table I. The foams were made in a box-foaming operation where the polyol, water, surfactant (TEGOSTAB BF-2370), and amine catalyst (DABCO 8264) were initially combined followed by the tin catalyst (T-9) and finally the TDI. A 2700 molecular weight proprietary polyol with a 3.15 nominal functionality and secondary hydroxyl groups was used in this study. Figure 1 illustrates the basic reactions involved in the production of polyurethane foams and the resultant morphological model. The reaction products of the blowing reaction between the TDI and water are carbon dioxide (which foams the reacting mixture) and a disubstituted amine. A relatively high water content (6 pph) is used to produce low density foams without the use of auxiliary blowing agents, provided that sufficient isocyanate is added to react with the water. The amine generated in this reaction as a by-product reacts with additional isocyanate to produce high T_g rigid urea groups that, given a sufficient concentration, phase separate into domains (hard seg-

Table I Formulation Components of Slabstock Foams Varying in TDI Index

Component	F85	F90	F95	F100	F105	F110
Polyol	100	100	100	100	100	100
H_2O	6	6	6	6	6	6
BF-2370	1.1	1.1	1.1	1.1	1.1	1.1
DABCO-8264	0.12	0.12	0.12	0.12	0.12	0.12
T-9	Varied accordingly					
TDI index	85	90	95	100	105	110
TDI amount	57.9	61.3	64.7	68.1	71.5	74.9
Density (pcf)	1.25					

The values in the table designate the formulation amounts in terms of pph by weight of polyol. The functions of each of the chemicals listed above are as follows: polyol, 2700 molecular weight triol utilizing sucrose–glycerol initiator blend; water, blowing agent; TDI, a blend of isomers of toluene diisocyanate; BF-2370, a silicone surfactant; T-9, a tin catalyst commonly known as stannous octoate; DABCO 8264, tertiary amine primarily a blowing catalyst; and TDI, a blend of isomers of toluene diisocyanate.

ment domains) that are primarily due to hydrogen bonding with additional urea groups. This is illustrated in Figure 1 by the simplified and somewhat idealized two phase model that unrealistically neglects imperfections in the hard segment domains such as disorder and the hard segments found in the soft phase. These domains are commonly referred to as physical crosslinks because they enhance the physical properties at room temperature and low humidity. At elevated temperatures and humidities, these physical crosslinks are significantly labile to alter the properties of the foams. The hard segment domains (structure, order, concentration) play a very important role on the final structure, morphology, and properties of the foam.

The reaction product between the isocyanate and multifunctional polyol is a urethane group that links the urea groups to the ether soft segments and provides a covalently crosslinked network. Two secondary reactions can also occur provided excess isocyanate is available and there are high temperatures, both of which are true in this case for the high index foams and high water content. The first reaction is between a urea group produced in the blowing reaction and an additional isocyanate group giving a biuret. In a similar manner the second is between a urethane group produced in the gelling reaction and an isocyanate group giving an allophanate. Both reactions can further covalently crosslink the polymer.

Methods

The cellular structure of these foams was evaluated and compared using scanning electron microscopy (SEM). Thin slices (3–4 mm) of foam were adhered to aluminum stubs using silver paint and then allowed to dry. A thin layer of gold was then applied to the surface of the foam using an SPI model 13131 sputter coater. Micrographs were taken using a Cambridge Stereoscan model 100 operating at 20 kV and at a magnification of approximately 30×.

Extraction experiments were carried out on selected samples for the purpose of comparing the relative level of crosslinking as a function of TDI index. Samples of various shapes and sizes ($<$0.15 g) were cut from the center of the foam bun, dried, and weighed. The samples were submerged in DMF (ca. 10× by volume) for a period of 48 h. The samples were then removed from the DMF and dried under a vacuum at 40°C for approximately 24 h and finally at 80°C for approximately another 48 h. The weight of the samples was measured at increments throughout the drying process.

Tensile stress–strain measurements were conducted using an Instron model 1122 equipped with pneumatic grips and linked to a computer with an in-house program written in Basic for data collection. The dogbone-shaped samples had dimensions of 2.8 × 6.7 × 24 mm with a grip to grip distance of 10 mm stretched at 0.15 mm/min.

Load relaxation experiments were performed using a procedure similar to that used and described by Moreland et al., which was originally designed to mimic the ASTM procedure used for IFD testing.[7] Samples of dimensions 3.5 × 3.5 × 1 in. were cut from the molded foam bun using a band saw equipped with a wavy edge saw blade. Each sample was first dried under vacuum and at 40°C for 3.5 h to give each sample an equal level of moisture. The samples were then placed in an environmental chamber preset at the testing conditions for ca. 60 min. The environmental

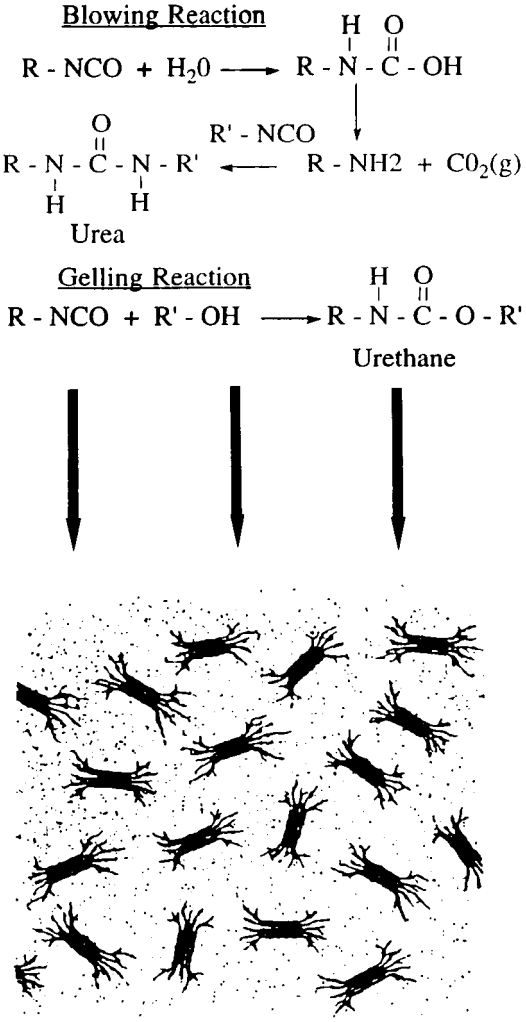

Figure 1 Basic reactions and general resultant morphology involved in flexible slabstock polyurethane foams.

chamber was purchased from Russells Technical Products and was equipped with a Watlow 922 microprocessor that controls temperature in the range of 20–300°C and humidity in the range of 0–100%. The chamber was fit into the Instron frame equipped with a model MDB-10 compression load cell manufactured by Transducer Techniques. Using a 2-in. indentor, initially at rest the samples were compressed and released twice to 70% at a rate of 350 mm/min. After 5 min the samples were compressed to 65% strain at which point the load was immediately monitored via computer. The onset of densification for polyurethane foams in the density range studied here occurs at approximately 65% where relaxation occurs within the solid polymer independently of cellular structure.

Compression set experiments were carried using a non-ASTM procedure that reflected the load relaxation measurements. The samples were cut into dimensions of 50 × 50 × 25 mm and dried under a vacuum for approximately 3.5 h. They were then placed in the environmental chamber at the designated environmental conditions for ca. 1 h following which they were compressed to 65% for 3 h. The samples were then removed and placed in an oven at 40°C after which dimensional measurements were made. Recovery measurements were carried out on the samples that displayed the greatest amount of compression set that occurred at the highest temperature and humidity condition (100°C and 98% relative humidity, RH). After about one month of further room temperature storage, these samples were placed in a oven at 100°C for 1 h. The foam thickness was measured and recorded.

Phase separation was in part evaluated using SAXS scans obtained with a Phillips model PW1729 generator operating at 40 kV and 20 mA. The smeared data were collected using a Kratky camera, with nickel filtered CuKα radiation having a wavelength of 1.542 Å passing through a slit collimator (0.03 × 5 mm). The detector used was a Braun OED 50 position-sensitive platinum wire detector. The raw data were corrected for parasitic scattering and normalized for thickness variation using a Lupolen standard. The foam samples were cut approximately 10-mm thick and compressed to approximately 3 mm.

DSC was used to obtain a qualitative indication of the level of phase separation using a Seiko model 5200. The samples were first cooled to −140°C and then heated to 140°C, held there for 5 min, cooled again to −140°C, and finally heated again to 140°C, all at 10°C/min. Attention was paid to shifts in the glass transition as a function of index as well as the DSC signal before and after this transition. The latter can be correlated to the specific heat change below and above the T_g.

Dynamic mechanical analysis (DMA) was carried out using a Seiko model 210 in the tension mode. The samples were heated from −100 to 140°C at a rate of 1°C/min, from which storage modulus (E') and tan δ data were collected at a frequency of 1 Hz. The sample dimensions were approximately 6.8 × 6.8 × 25 mm with a grip to grip distance of 10 mm. The maximum in the tan δ curve, used as an indication of the glass transition, was followed as a function of index.

FTIR was used to assess the relative degree of order of the hard segments as a function of index on a Digilab FTS-40 spectrophotometer equipped with an ATR cell. For each sample 64 scans were

averaged that were taken in the range of 4000–400 cm^{-1} with a resolution of 4 cm^{-1}. All scans were normalized to the absorbance of a CH stretch at 2945 cm^{-1}. The regions studied were the amide I region (1620–1800 cm^{-1}), the N—H region (3100–3500 cm^{-1}), and the isocyanate region (2200–2400 cm^{-1}).

In studying the degree of order within the hard segments, wide angle X-ray scattering (WAXS) patterns were obtained as a function of index. The X-ray source was a Philips X-ray generator model PW1720 using a Statton camera and a fine focus tube with nickel filtered CuKα radiation having a wavelength of 1.542 Å. Foam samples were cut approximately 10-mm thick and compressed to approximately 3 mm. The sample to film distance was 8 cm and exposure times were 10 h.

RESULTS AND DISCUSSION

SEM Observations

Scanning electron micrographs were taken of the foam samples to observe any distinct differences in the cellular structure as a function of index that can inherently influence their mechanical properties. Figure 2(a,b) shows two micrographs, one of F85 and one of F110. Evaluation of these micrographs leads to the conclusion that the cellular structures were relatively unaffected by altering the TDI index. As can be observed, both micrographs show that while both foams are open celled, they each have a considerable amount of closed cells. Evaluation of micrographs of the intermediate TDI index foams revealed the same type of cellular structure and are thus not shown. Therefore, differences in the physical properties between the foams as a function of index are not likely a result of different bulk cellular structures. Micrographs were also taken of the same two samples given in Figure 2 after extraction to observe their resistance to cell structural changes induced by DMF used as the extraction medium. Figure 3(a) is a micrograph of F85 after extraction. As can be seen, the extraction process has promoted dramatic structural changes that have caused the foam to essentially collapse into a much more dense filmlike material. In a similar manner, Figure 3(b) presents a micrograph of F110 after extraction. In this case, after extraction the foam is only partially altered but the cellular structure is still quite similar to its unextracted form. The previous two figures further support the claim that the different TDI indexes have direct correlation to the level of covalent crosslinking as will be directly supported below by the results of the extraction studies.

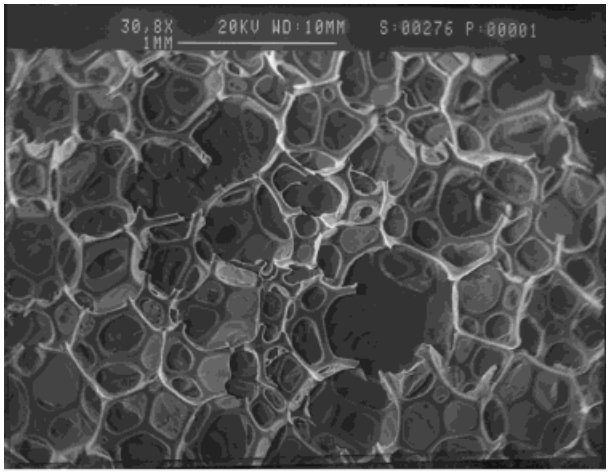

(a)

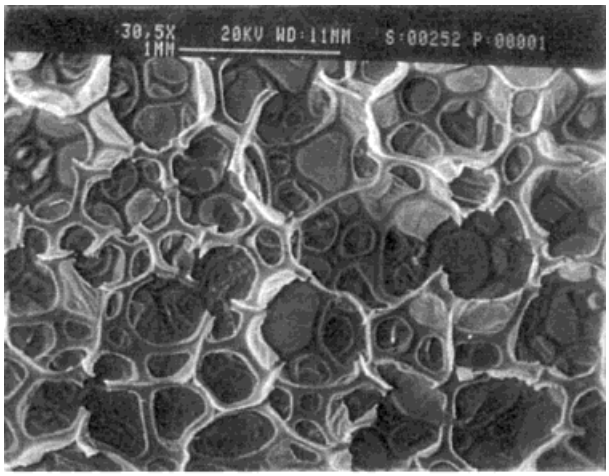

(b)

Figure 2 Scanning electron micrographs of foam samples (a) F85 and (b) F110 shown at an original magnification of 30×.

Solvent Extraction Results

Results from the 48-h extraction studies are given in Table II. Four of the six foams were chosen for this experiment from which the results can be qualitatively related to the amount of crosslinking. As can be seen from Table II, F85 displayed a sol fraction of ca. 32%. As the TDI index was increased, the amount of extractables decreased, suggesting that the amount of covalent crosslinking increased. However, it also appears from these results that at an index of 100 or above that the

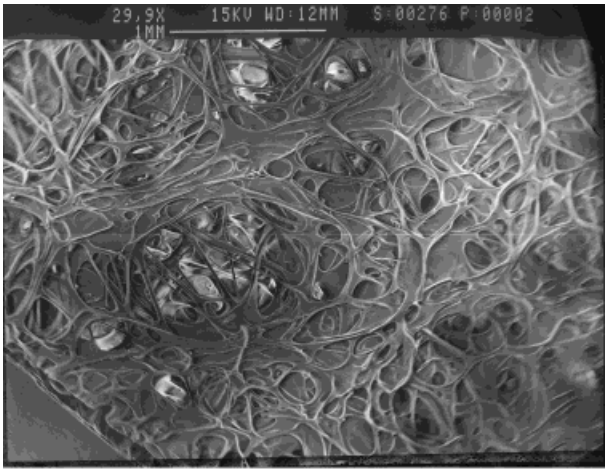

(a)

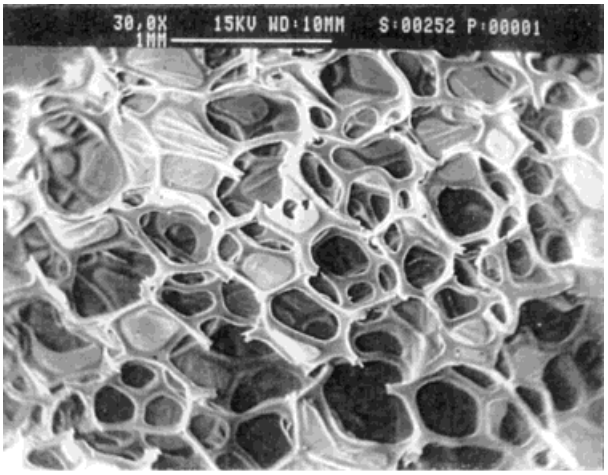

(b)

Figure 3 Scanning electron micrographs of foams following extraction process: (a) F85 and (b) F110.

sol fraction (and thus the gel fraction) remains essentially constant. Traditionally, an offset in stoichiometry at the time of polymerization results in a decrease in molecular weight and lower crosslink density. However, in view of the possibility for biuret and allophanate formation in urethanes, over-indexed polyurethanes can, if conditions and suitable catalysts such as potassium octoate are utilized, lead to an increased crosslink density let alone a higher hard segment content. It can be concluded from these results that increasing the TDI index does increase the covalent crosslinking to an extent. Therefore, to further evaluate the influence of this crosslinking and the physical crosslinks as a function of index, viscoelastic measurements were undertaken.

Table II Percent Sol from Solvent Extraction Studies Using DMF

Foam	Sol Fraction (%)
F85	31.3 ± 0.5
F90	15.0 ± 0.6
F100	5.6 ± 0.5
F110	6.0 ± 0.4

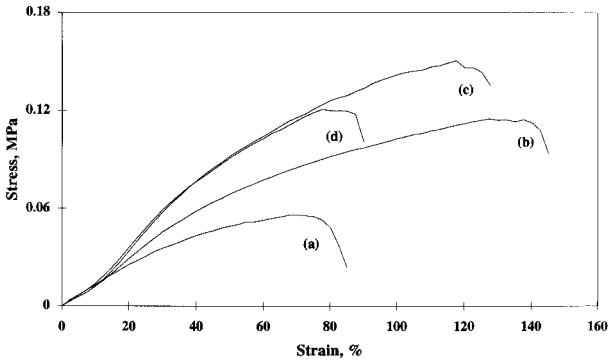

Figure 4 Tensile stress–strain behavior for the foams (a) F85, (b) F100, (c) F105, and (d) F110.

Mechanical and Viscoelastic Behavior

Tensile stress–strain results for the same four foams used for the extraction studies are shown in Figure 4. First the modulus (ca. 0.1 MPa) appears to be insensitive to TDI index up to approximately 15% strain, beyond which an increase in index leads to an increase in stress as a function of strain. Additional tests of other samples revealed the same behavior in that the modulus did not change with TDI content for the conditions utilized. As is well known, the hard segment domains as well as the covalent crosslinking strongly influence the mechanical properties; however, here both are being influenced in opposing ways and the apparent result is that no significant change occurs in the Young's modulus. Gibson and Ashby[8] related the modulus of a foam to the modulus of the solid portion as well as the reduced density,

$$E_f = C_1 E_s \left(\frac{\rho_f}{\rho_s} \right), \quad (1)$$

where E represents the modulus, ρ represents the density (the subscript s denotes the solid portion while f denotes the foam), and C_1 is a constant. A speculation is that the small change E_s in the

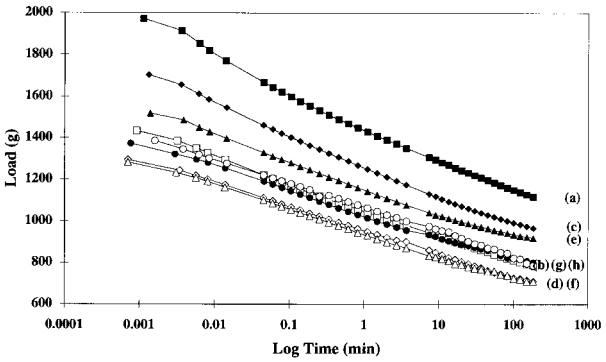

Figure 5 Load relaxation behavior of F85 as a function of temperature and relative humidity: (a) 30°C and 35% RH, (b) 30°C and 98% RH, (c) 50°C and 35% RH, (d) 50°C and 98% RH, (e) 80°C and 35% RH, (f) 80°C and 98% RH, (g) 100°C and 35% RH, and (h) 100°C and 98% RH.

solid portion modulus within the index range studied may not be reflected in the foam modulus, E_f due to its behavior being offset by the variation of the relative modulus, that is, an increase in the density of the solid portion, ρ_s. Another likely variable behind the insensitivity of the modulus to the index is that the TDI content in even the lowest index foam is still above the 57% weight level. Following foam development, as a result there will be continuity of hard domain textures that will help mask the effects on stiffness to further TDI content. Interestingly, an insensitivity to crosslinking of the foam modulus was also observed by Thomas et al.[4] The effect of the index is, however, more pronounced at strain levels beyond 15%. Both the stress at failure and strain at failure displayed a maximum at an index of 100 (F100). Foam F110 followed the same curve as F100 up to 75% strain where it failed. The maximum displayed by F100 may be in part due to an increase in the concentration of urea groups and thus hard segment domains over that of lower index foam samples in addition to increased crosslinking. The decrease in extensibility exhibited by foam F110 may be in turn due to a further increase in the level of crosslinking and HS content, thereby providing a "tighter" network.

The viscoelastic behavior can be used to address durability, recoverability, and long-term behavior of these materials. Therefore, both the compression creep and load relaxation behavior was measured to evaluate the influence of the physical crosslinks as well as covalent crosslinks for this series of varying TDI index foams. Compression load relaxation was investigated at four temperatures (30, 50, 80, and 100°C) and two relative humidities (35 and 100%) for each of the six foams. Figure 5 illustrates the load relaxation behavior for foam F85 as a function of temperature and humidity. At 30°C and 35% RH, the initial load was 1973 g but decayed 43% to 1125 g in the 3-h testing period. As can also be seen from Figure 5, increasing the temperature and/or relative humidity systematically shifted the relaxation curves to lower loads. The initial load decreased from 1973 g at 30°C and 35% RH to 1373 g at 100°C and 35% RH while the percent decay remained roughly constant at 43% in a 3-h experiment. Similar behavior was observed at 98% RH. At a constant temperature, an increase in humidity from 35 to 98% RH also had a distinct "softening" effect. For example, the initial load decreased from 1973 g at 30°C and 35% RH to 1435 g at 30°C and 98% RH. Interestingly, the authors found by similar studies that the moisture softening effect is greater in molded foams than in conventional slabstock foams.[9] This "plasticization" has traditionally been attributed to the disruption of hydrogen bonds by temperature and/or humidity. Hydrogen bonding is reported to occur predominantly within the hard segment domains and to some extent between urea or urethane linkages with the ether groups within the soft segment. The degree of plasticization that occurs with temperature and humidity is evidence suggesting that the virtual crosslinks play a very significant role in the properties of the foam at ambient conditions.

Shown in Figure 6 are the load relaxation results as a function of temperature and humidity for F110. The temperature and humidity effects are similar to F85 but the initial loads are greater

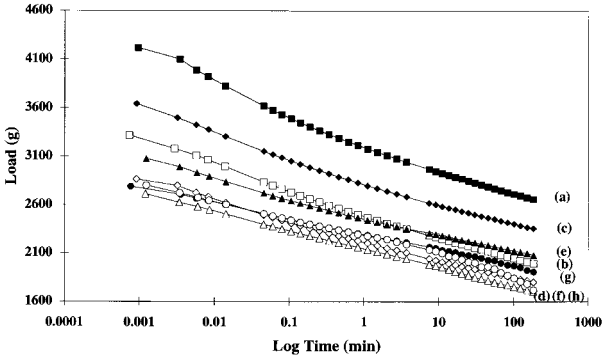

Figure 6 Load relaxation behavior of F110 as a function of temperature and relative humidity: (a) 30°C and 35% RH, (b) 30°C and 98% RH, (c) 50°C and 35% RH, (d) 50°C and 98% RH, (e) 80°C and 35% RH, (f) 80°C and 98% RH, (g) 100°C and 35% RH, and (h) 100°C and 98% RH.

Table III Summary of Load Relaxation Results for Three Foam Samples

	Temperature (°C)	RH (%)	Initial Load (g)	Decay (%)	SD (±g)
F110	30	35	4218	37.1	102
	100	35	2899	31.6	82
	30	98	3319	40.0	74
	100	98	2799	38.5	21
F100	30	35	3490	39.9	26
	100	35	2847	29.2	50
	30	98	3053	39.6	156
	100	98	2420	39.0	71
F85	30	35	1973	43.3	40
	100	35	1373	41.7	39
	30	98	1435	45.5	30
	100	98	1387	43.4	20

and percent decays are lower for F110, suggesting that this foam is a less time-dependent foam than F85 as would be expected. The percent decays are summarized in Table III. The range for F85 was 42–46% while for F110 the range was 32–40%. As with the low index foam, temperature and/or humidity also plasticized the load relaxation behavior for F110 as expected. At 30°C and 98% RH and 100°C and 98% RH the initial loads were 3319 and 2799 g, respectively. The plasticization with temperature and/or humidity suggests that hydrogen bonding and thus the virtual crosslinks *still* play a very significant role in the properties while the increased loads and decreased decays suggest that the increased TDI index is "tightening" the network. The remaining four foams of intermediate index displayed intermediate behavior (with respect to temperature and/or humidity) to these two extremes.

The remaining load relaxation data are displayed in Figures 7–9 as a function of index at a given temperature and humidity. For example, Figure 7 shows the load relaxation results at 30°C and 35% RH for all six foams. In general, an increase in index shifts the curves toward higher loads. The initial loads increased and the percent decays decreased and are also displayed in Table III that lists the initial loads, percent decays, and standard deviations for three of the foams. Although there is some scatter in the data and therefore some overlap in the standard deviations, a trend of shifting the curves to higher loads with increasing index is clearly illustrated in Figure 7. Figure 8 shows the load relaxation results of the six foams at 100°C and 35% RH. The trend is again the same in that the curves lie in systematic order of increasing index with the exception of the two foams F105 and F110, which are essentially indistinguishable. Similar behavior between these two foams was observed throughout this relaxation study, suggesting that there is little difference between the two. A major difference

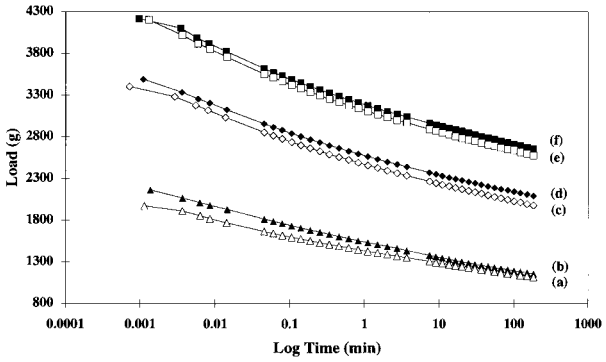

Figure 7 Load relaxation behavior at 30°C and 35% RH of the foams varying in index: (a) F85, (b) F90, (c) F95, (d) F100, (e) F105, and (f) F110.

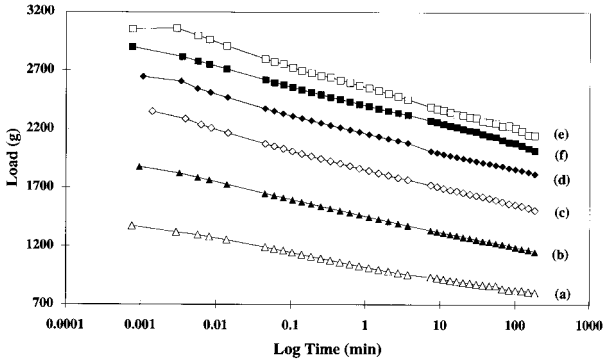

Figure 8 Load relaxation behavior at 100°C and 35% RH of the foams varying in index: (a) F85, (b) F90, (c) F95, (d) F100, (e) F105, and (f) F110.

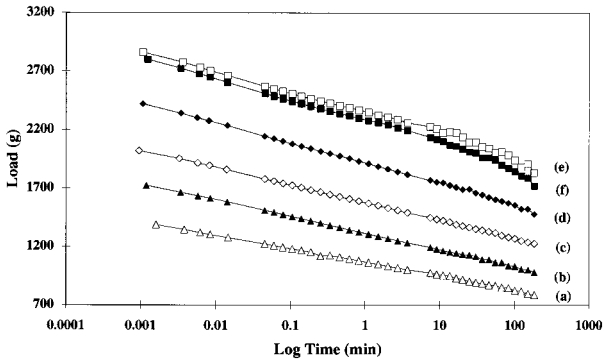

Figure 9 Load relaxation behavior at 100°C and 98% RH of the foams varying in index: (a) F85, (b) F90, (c) F95, (d) F100, (e) F105, and (f) F110.

between the results at 100°C and 35% RH and at 30°C and 35% RH is that the former relaxation curves have been shifted to considerably lower loads. Finally, Figure 9 shows the load relaxation behavior at 100°C and 98% RH and the trend with index is consistent with the results at the other conditions, including the indistinguishability between the two high foams F110 and F105. It is noted that for these conditions the initial loads have been dramatically decreased with respect to what was observed at ambient conditions. In addition, the curves deviate from linearity compared to the curves at 30°C and 35% RH, indicating that the relaxation process may be a result of an additional mechanism or just a rate enhancement of the same mechanism. It can be concluded from the load relaxation results that increasing the TDI index significantly increased the stiffness, suggesting that indeed the covalent network structure as well as the hard segment content are enhanced further by increasing the TDI amount. This may be surprising because, *based on stoichiometry, an offset typically reduces the effective elastic chain concentration.* Also, because the 2,4-TDI reacts more slowly than the 2,6-TDI, the use of a higher index helps to provide a sufficient level of reaction to offset any loss in network formation caused by unreacted isocyanate groups. In addition, due to the high exotherms and the availability of amine groups, some formation of biurets and allophanates is also possible, thereby providing increased crosslinking as well as the presence of additional hard segment reactant.

To further evaluate the covalent and physical networks as influenced by the index, another viscoelastic measurement was undertaken. Compression set experiments were also utilized to evaluate the recoverability of a given foam after having been compressed for a certain length of time under specified environmental conditions. The compression set results for the F85, F100, and F110 foams are presented in Table IV that shows the amount of compression set induced to the samples compressed to 65% at the various environmental conditions for 3 h. Surprisingly, there appears to be very little influence on the compression set by the TDI index. As expected, however, increasing the temperature and/or relative humidity increased the amount of compression set. The independent behavior of the compression set relative to the index may be explained in terms of the compression set being influenced by both the virtual crosslinked hard segment domains and the covalent crosslinks, both being altered by the varying TDI index. It may be feasible that a sufficient concentration of virtual crosslinks may be responsible for this independence. When comparing the *thermally* induced recovery results (at 100°C), however, the effect of the TDI index is very significant as shown in Figure 10. The higher fraction of covalent elastically active chains in the higher index foams allow the foam to recover toward its original state once the hydrogen bonds are softened at 100°C. The fact that as the index is increased, the amount of recovery is also significantly increased is strong evidence supporting the previously shown results of increased covalent crosslinking.

Table IV Compression Set Results of Foams Varying in TDI Index

Condition	F85	F100	F110
30°C, 35% RH	1.7 ± 0.0	2.5 ± 0.2	2.2 ± 0.1
30°C, 98% RH	3.8 ± 0.3	5.3 ± 0.3	5.1 ± 0.5
100°C, 35% RH	15.2 ± 1.6	12.2 ± 2.0	12.0 ± 0.5
100°C, 98% RH	54.8 ± 1.4	55.4 ± 1.8	56.4 ± 1.2

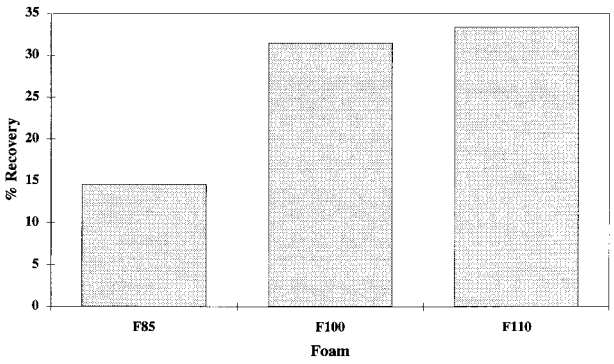

Figure 10 Compression set recovery as a function of index.

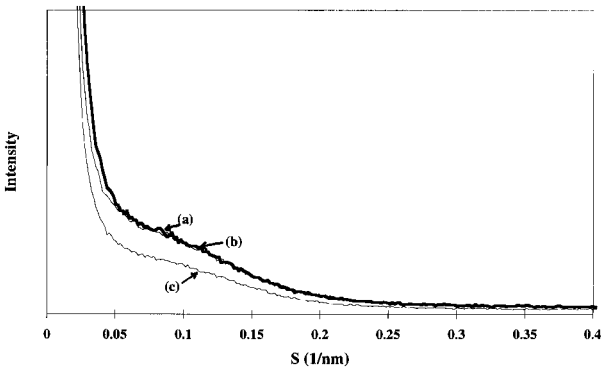

Figure 11 SAXS profiles of slabstock polyurethane foams (a) F85, (b) F100, and (c) F110 illustrating the influence of TDI index on the microphase separation.

Morphological Characterization

From the physical property measurements it was concluded that altering the amount of TDI added in the formulation had significant consequences on these properties and more directly on the network structure. In addition to its influence on the physical properties, it was of interest to investigate how varying the TDI index affects the domain texture of the polyurethane foams. SAXS, a technique used for studying microphase separated polymers, was carried out to observe the presence of phase separation and how it was affected by the index level. Figure 11 shows the normalized smeared intensity $\tilde{I}(s)$ as a function of an angular variable or scattering vector $\mathbf{s}$ where $\mathbf{s} = 2 \sin \theta/\lambda$ (reciprocally related to the Bragg spacing) for foams F85, F100, and F110. Although not well pronounced, a very weak broad shoulder does consistently occur ($\mathbf{s} \approx 0.1\ \mathrm{nm}^{-1}$), signifying phase separation and from which an estimated characteristic distance between the scattering centers, or Bragg spacing, can be extracted, that being ca. 100 Å. Also observed in Figure 11 is that the measured intensity of F85 is higher than that of F110. The increased crosslinking with increased index level prevented phase separation from occurring *to the extent it occurs in foam F85.* This was concluded based on the simplified interpretation of the scattering invariant that, for an ideal two phase system with sharp boundaries, is given as

$$\overline{\Delta\rho}^2 \approx \varphi_1\varphi_2[\rho_1 - \rho_2]^2 \qquad (2)$$

where ϕ_1 and ϕ_2 are the volume fractions of each phase and $[\rho_1 - \rho_2]$ is the electron density difference between the two phases. As is clear from eq. (2), for a given value of $[\rho_1 - \rho_2]$, the invariant achieves a maximum when each volume fraction is 0.5. As the volume fractions deviate from 0.5, the invariant decreases. Thus, an estimation of the amount of phase separation can be obtained by comparing the theoretical invariant to the experimentally determined invariant by

$$\overline{\Delta\rho}^2 \approx \frac{2}{V}\int_0^\infty \tilde{I}(s)s^2\,ds \qquad (3)$$

where $\tilde{I}(s)$ is the smeared scattered intensity. Therefore, by taking a ratio of the experimentally determined and theoretically calculated invariant, a qualitative estimate of the degree of phase separation can be obtained. While this quantitative analysis was not carried out, the direct observation of the results presented in Figure 11 of the normalized intensity also visually indicate that the invariant (related to a function of the area under the scattered intensity profile) for foams F85 and F100 is higher than for F110, suggesting that even though the HS content increases with increasing index (up to 100 index), at the highest index level more hard segments are solubilized within the soft phase, thereby lowering the overall scattering intensity. Again, the data were only normalized and treatments such as desmearing, and background removal have not been undertaken. However, it is believed that this type of treatment would not greatly influence the *trend* demonstrated by the data as presented. Therefore, the SAXS results at least qualitatively impart that the extent of microphase separation decreases as the covalent crosslinking increases above the TDI index of 100.

The results of the SAXS experiments were confirmed using another technique, DMA. DMA was carried out to follow the change in T_g, determined as being the peak in the tan δ curve, with altered TDI index. The tan δ results for the four foams are shown in Figure 12. As can be seen, the soft

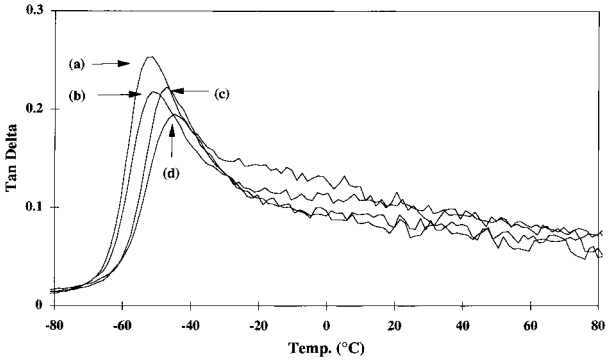

Figure 12 Influence of the TDI index on the tan δ peak: (a) F85, (b) F95, (c) F100, and (d) F110.

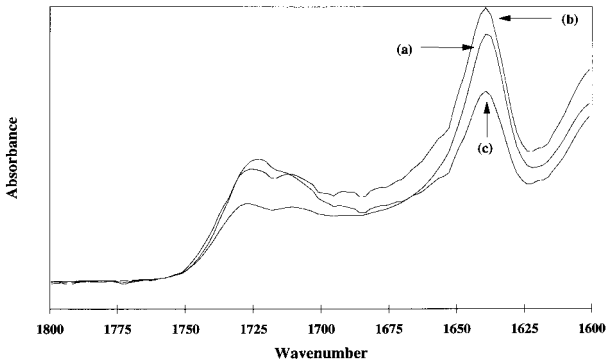

Figure 13 Influence of TDI index on the bidentate absorbance in the FTIR spectra of foams (a) F85, (b) F100, and (c) F110.

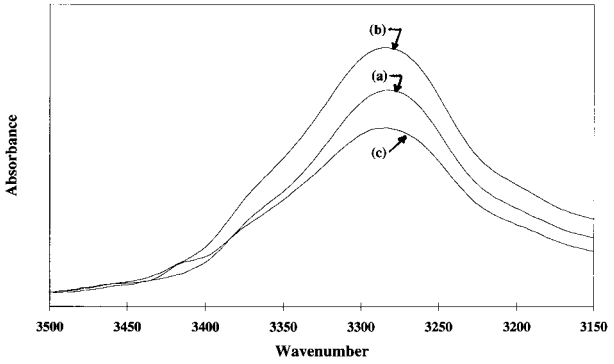

Figure 14 Influence of TDI index on the NH absorbance in the FTIR spectra of foams (a) F85, (b) F100, and (c) F110.

segment T_g shifts toward higher temperatures with increasing index value. The T_g values are −53°C for F85, −51°C for F95, −48°C for F100, and −45°C for F110. In addition, the decreasing magnitude of the tan δ peak further indicates that the material is "stiffer" above the soft segment T_g as expected due to a lesser volume fraction of polyol with increasing index. The shift in T_g to higher temperatures, however, indicates phase mixing.

FTIR spectroscopy was used to study the ordering of the hard segments by studying the hydrogen bonding in the carbonyl and N—H regions.[10] The FTIR spectral profiles for the F85, F100, and F110 foams are shown in Figure 13. The bidentate peak centered at about 1640 cm^{-1} shows that the ordering within the hard segments goes through a maximum as a function of index similar to the behavior observed by Skorpenske et al.[6] Foam F100 shows a stronger bidentate peak than F85, which is believed to be due to a higher concentration of well-ordered hard segment domains. This behavior strongly suggests that the development of hard segment domains is further enhanced with initial increases in index (up to ca. 100 index). The bidentate peak absorbance for F110 is dramatically lower than either F100 or F85 due to a disruption of the hard segment ordering by the increased covalent crosslinking. That is, the increased covalent crosslinking that occurs in this high index foam makes it more difficult for the urea segments to associate (through diffusion) and to pack well with other hard segments, thereby limiting perfection of the hard segment domains with bidentate hydrogen bonding that must principally occur prior to the covalent gel point. Although the nonbonded urea and urethane, centered at ca. 1695 and 1730 cm^{-1}, respectively, appear to increase with increasing index, it is difficult to conclusively confirm this due to the convoluted nature in this region (1695–1750 cm^{-1}). This is due to the fact that contributions from free urea groups, bonded urethane groups, free urethane groups, allophanate groups, and biuret groups all absorb here. The trend in the N—H absorbance region shown in Figure 14 is similar to that in the carbonyl region. The hydrogen-bonded N—H absorbance centered at about 3280 cm^{-1} is highest for F100 and lowest for F110 with the absorbance for F85 lying between. As stated earlier, this is believed to be due to F100 (85 index) having the highest concentration of well-ordered hard segment domains while the additional crosslinking in F110 is disrupting the hard segment ordering or perfection of the domains. Figure 15 shows the FTIR spectral profiles of the three foams in the isocyanate region. Not surprisingly, this figure shows an increase in the amount of free isocyanate, suggesting that as the

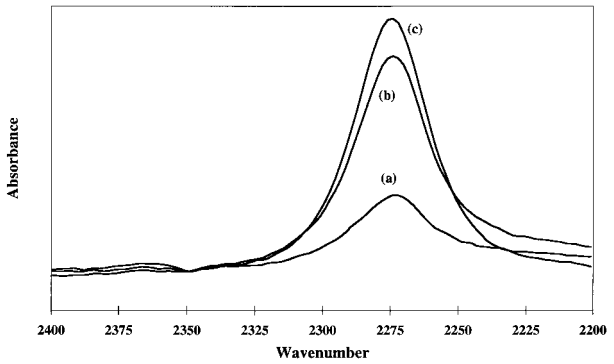

Figure 15 Influence of TDI index on the free isocyanate absorbance in the FTIR spectra of foams (a) F85, (b) F100, and (c) F110.

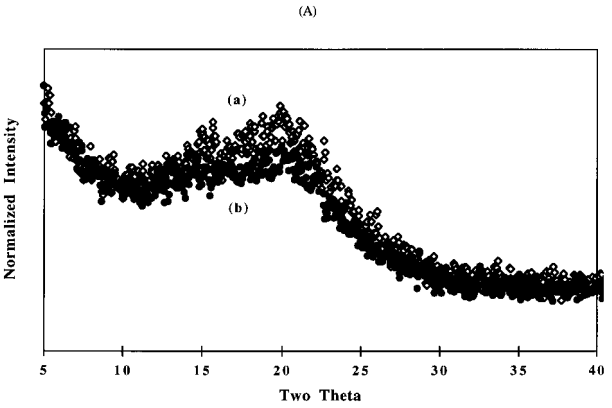

Figure 16 WAXS diffractometer scans illustrating the influence of TDI index on the short-range ordering of the HS domains: (a) F85 (◇), (b) F110 (●).

TDI index is increased; the amount of unreacted isocyanate is also increased.

It is recalled from the section on experimental procedures that the FTIR absorbances were normalized in the CH based at 2945 cm^{-1}. Because nearly a 9% difference exists in CH content exists and varies across the index range studied, this would, of course, promote some differences in the FTIR spectra between the different index forms. However, this difference would not negate the trends discussed above because the observed changes are far in excess of this 9% difference.

The short-range ordering or organization of the hard segment domains was also studied using WAXS. The WAXS diffractometer scan, which is a plot of intensity versus the scattering angle 2θ, for foam F85 is shown in Figure 16 as is also the scan of foam F110. Both show two peaks having a corresponding Bragg spacing of approximately 4.5 and 6.0 Å. The exact origin of these peaks is unknown but has been clearly attributed to the organized or paracrystalline hard segment ordering through hydrogen bonding.[11] The sharpness and intensity of the peaks can be used to qualitatively assess the level of ordering of the hard segments. The peaks (esp. 6.0 Å) are sharper and of higher intensity for F85 than for F110, which is attributed to a lowering of the hard segment ordering by the additional covalent crosslinking in F110. The limitations on the molecular packing by the additional crosslinking decrease the domain cohesiveness, which can allow for the easier plasticization by temperature and/or humidity. For example, comparing the load relaxation behavior at 100%°C and 35% RH (Fig. 8) of F105 to F110 reveals that F105 displayed stiffer behavior than F110. The WAXS results clearly support the FTIR conclusions that increasing the TDI index disrupts the ordering of the hard segment domains.

CONCLUSIONS

Flexible slabstock polyurethane foams were produced using a high water content formulation without the use of auxiliary blowing agents and varying levels of TDI to influence the softness of the foams. As the TDI index was increased, the hardness at a 65% compression of the material also increased, suggesting that the higher index in the formulation resulted in a higher hard segment content and/or a higher covalent network. Solvent extraction experiments indicated that covalent crosslinking was a direct consequence of altering the TDI index. The amount of extract decreased systematically with increasing index. However, there was essentially no significant difference in the extractability between the 100 index foam and the 110 index foam, suggesting that the amount of crosslinking reached a maximum at about a 100 index. It is again recognized, as stated earlier, that depending on the reactivity of the TDI isomers (as well as the functionality of the polyol), the index value of 100 may well not always be expected to provide the highest level of crosslinking.

The mechanical and viscoelastic properties also complimented the above findings. The stress and elongation at break increased as a function of index, with the exception of the highest index where the strain to break was much lower. The initial loads systematically increased with increasing index with the exception of the two highest index foams. Likewise, the percent decays systematically decreased with increasing TDI index. All foams were significantly softened by either temperature or humidity and especially by a combination of both variables. While the compression set properties appeared to be independent of TDI index, the different TDI indices were clearly evident in the recovery of the compression set experiments. As the temperature was increased to induce recovery, higher recovery from the compression set was achieved for the higher index foams in a systematic fashion. The increasing recovery with increasing index is attributed to and viewed as strong evidence for the direct correlation between the TDI index and covalent crosslinking.

Along with investigating the influence of the index on the physical properties of polyurethane foams and in an effort to understand the fore-

mentioned observations, we investigated its effect on morphology of these materials as well. SAXS results qualitatively indicated that the lowest index foam had better phase separation than the highest index foam. This was supported by DMA measurements where the observed soft segment glass transition region increased in temperature with increasing index.

The level of short-range ordering of the hard segments was studied by FTIR and WAXS. FTIR indicated that the amount of well-ordered bidentate urea decreased at indices either above or below an index of 100. The 100 index foam displayed the highest amount of bidentate, suggesting this material has the highest concentration of well organized hard segments. This evidence strongly supports the claim that the increased covalent crosslinking decreases hard segment domain perfection. WAXS results confirmed this claim that showed that increasing the index caused the short-range order of the hard segments to decrease.

The authors wish to thank Dow Chemical U.S.A. for their financial support and for the foam samples. We would also like to acknowledge Professor Eva Marand for use of her IR equipment.

REFERENCES

1. Z. S. Petrovic, M. Ilavsky, K. Dusek, M. Vidakovic, I. Javni, and B. Banjanin, *J. Appl. Polym. Sci.,* **42,** 391 (1991).
2. Z. H. Ophir and G. L. Wilkes, *Adv. Chem. Ser.,* **176,** 53 (1979).
3. G. Spathis, M. Niaounakis, E. Kontou, L. Apekis, P. Pissis, and C. Christodoulides, *J. Appl. Polym. Sci.,* **54,** 831 (1994).
4. O. Thomas, R. D. Priester, Jr., K. J. Hinze, and D. D. Latham, *J. Polym. Sci., Part B: Polym. Phys.,* **32,** 2155 (1994).
5. K. D. Cavender and L. E. Hawker, 32nd Annual Polyurethane Technical/Marketing Conference, October 1989.
6. R. G. Skorpenske, R. Solis, R. A. Kuklies, A. K. Schrock, and R. B. Turner, 34th Annual Polyurethane Technical/Marketing Conference, October 1992.
7. J. C. Moreland, G. L. Wilkes, and R. B. Turner, *J. Appl. Polym. Sci.,* **52,** 549 (1994).
8. L. J. Gibson and M. F. Ashby, *Cellular Solids—Structure and Properties,* Pergamon Press, New York, 1988.
9. D. V. Dounis and G. L. Wilkes, unpublished manuscript.
10. J. V. McClusky, R. D. Priester, Jr., W. R. Willkomm, M. A. Capel, and M. D. Heaney, *Polyurethanes World Congress 1993,* 1993, p. 507.
11. J. P. Armistead, G. L. Wilkes, and R. B. Turner, *J. Appl. Polym. Sci.,* **35,** 601 (1988).